

Supporting Information

Takaki et al. 10.1073/pnas.0809674106

SI Text

CDK4/Cyclin D3 Purification. CDK4 and cyclin D3 were cloned into pFastBac1 (Invitrogen) with, respectively, GST and PreScission protease recognition sequences and a FLAG tag at the amino terminus. They were coexpressed in Sf-9 cells and purified by exploiting the CDK4 GST tag. Cells were harvested after 72 h of infection. Cell lysate was prepared by sonication followed by incubation in buffer A [50 mM Hepes (pH 7.5), 150 mM NaCl, 1 mM EDTA, 2.5 mM EGTA, 0.1% Tween-20, 10% glycerol, 1 mM DTT, and protease inhibitor mixture (Sigma)] for 30 min at 4 °C, and centrifugation at $70,000 \times g$ for 30 min at 4 °C. The supernatant was then incubated with 0.5 mL of glutathione Sepharose 4B (GE Healthcare) for 1 h at 4 °C. CDK4/cyclin D3 was eluted by buffer B [50 mM Hepes (pH 7.5), 150 mM NaCl, 2.5 mM $MgCl_2$, 1 mM EDTA, and 1 mM DTT] containing 20 mM glutathione, incubated with PreScission protease (GE Healthcare) for 3 h at 4 °C to cleave GST from CDK4, then dialyzed against buffer C [20 mM Hepes (pH 7.5), 150 mM NaCl, and 1 mM DTT] 3 times. The sample was incubated with 50 μ L of glutathione Sepharose 4B for 30 min at 4 °C and centrifuged, and in a final purification step, the CDK4/cyclin D3 complex was centrifuged through a Bio-Rad micro spin column.

CDK4/Cyclin D3 Characterization: Multiangle Laser Light Scattering. CDK4/cyclin D3 was applied to a Superdex 200 column ($K10 \times 300$; GE Healthcare) using an HPLC system equipped with an 18-angle MALLS detector (Dawn Helios II; Wyatt Technologies). BSA was used as a control. The protein concentration of the eluent was determined from the refractive index change ($dn/dc = 0.186$) by using an OPTILAB-rEX differential refractometer equipped with a Peltier temperature-regulated flow cell, maintained at 25 °C (Wyatt Technology). The wavelength of the laser in the DAWN-HELEOS and the light source in the OPTILAB-rEX were both 658 nm. The weight-averaged molecular weight of material contained in chromatographic peaks was determined by using ASTRA software version 5.1 (Wyatt Technology). Briefly, at 1-s intervals throughout the elution of chromatographic peaks the scattered light intensities together with the corresponding protein concentration were used to construct Debye plots [$KC/R\theta$ vs. $\sin^2(\theta/2)$]. The weight-averaged molecular weight was then calculated at each point in the chromatogram from the intercept of an individual plot. An overall average molecular weight and polydispersity term was calculated by combining and averaging the data from the individual measurements.

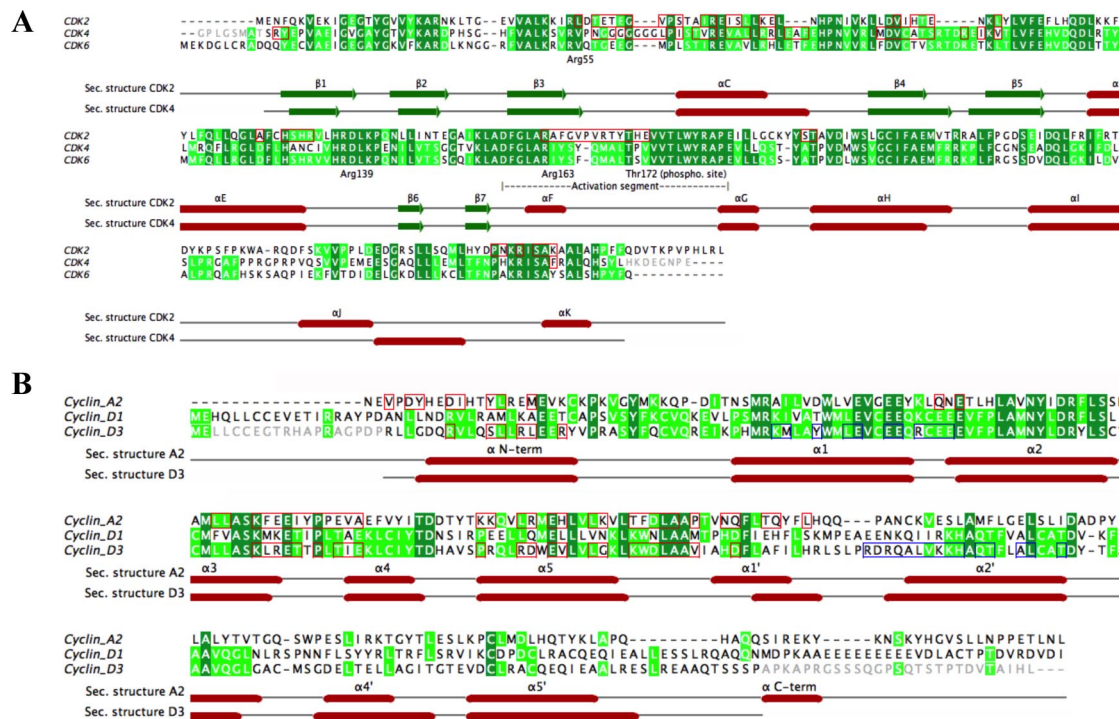
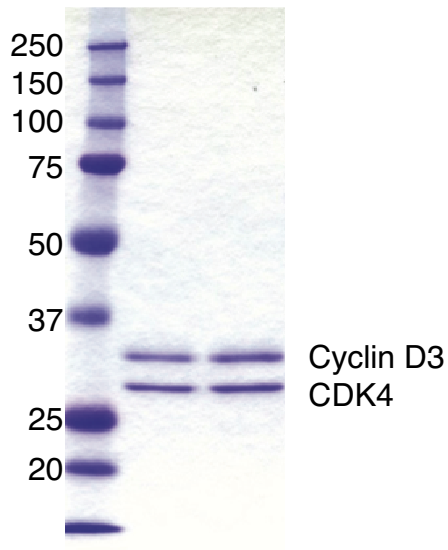


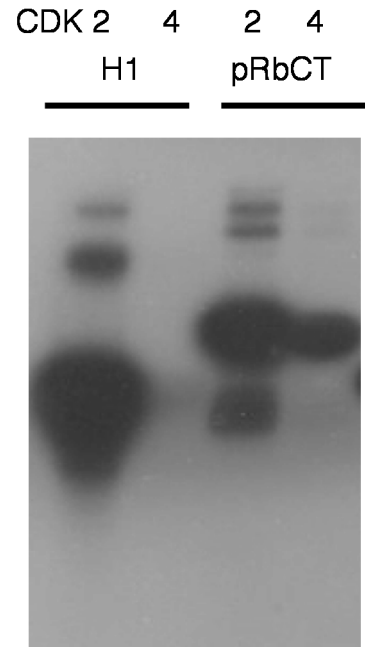
Fig. S1. Sequence alignments of CDK4 and cyclin D3. Selected human CDK and cyclin sequences were each aligned by using Jalview (1). The background to residues identical in all three sequences is dark green and to residues identical in any two sequences is lime. (A) CDK alignment. CDK sequences are CDK2 (Swiss-Prot entry P24941), CDK4 (P11802), and CDK6 (Q00534). CDK2 and CDK4 residues boxed in red compose the interface with cyclin A or cyclin D3, respectively. The three arginine residues in the CDK4 structure that are equivalent to CDK2 residues R50, R126, and R150 that compose the phosphoT160 binding site, T172 and the activation loop (the sequence between the DFG and APE motifs) are labeled. CDK2 and CDK4 secondary structural elements (α -helices in red and β -strands in green) present in the CDK2/cyclin A/substrate peptide (ref. 2; PDB ID code 1QMZ) and CDK4/cyclin D3 structures are drawn below the sequence alignment. (B) Cyclin alignment. Cyclin sequences are human cyclin A2 (Swiss-Prot entry P20248), cyclin D1 (P24385), and cyclin D3 (P30281). Residues boxed in red compose the CDK interface, and those in blue the cyclin D3/cyclin D3 interface. Red tubes below the sequences mark the positions of the α -helices in cyclin A2 and cyclin D3.

1. Clamp M, Cuff J, Searle SM, Barton GJ (2004) The Jalview Java alignment editor. *Bioinformatics* 20:426–427.
2. Brown NR, Noble ME, Endicott JA, Johnson LN (1999) The structural basis for specificity of substrate and recruitment peptides for cyclin-dependent kinases. *Nat Cell Biol* 1:438–443.

A



B



C

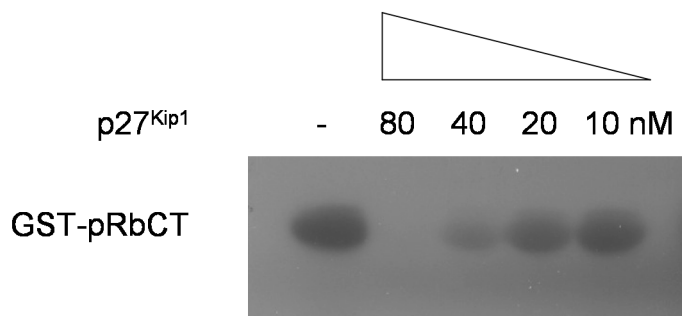


Fig. S2. Purification and characterization of CDK4/cyclin D3. (A) Purification of CDK4/cyclin D3. Selected fractions from the final size-exclusion chromatography step of the CDK4/cyclin D3 purification were subjected to SDS/PAGE analysis. At left, molecular mass markers are in kDa. The upper band in each CDK4/cyclin D3 sample is cyclin D3; the lower band is CDK4. (B) CDK4/cyclin D3 kinase activity. CDK4/cyclin D3 was assayed against histone H1 and a pRb fragment (see *Materials and Methods* for reaction conditions and construct details). CDK4/cyclin D3 shows robust activity toward the recruited substrate GST-RbCT but has no detectable activity toward histone H1. (C) p27^{Kip1} inhibition of CDK4/cyclin D3. CDK4/cyclin D3 (final concentration 90 nM) was coincubated with increasing quantities of p27^{Kip1}. Complete inhibition of CDK4/cyclin D3 phosphorylation of GST-pRbCT by p27^{Kip1} is observed at an approximately equimolar CDK/CKI ratio.

A

B

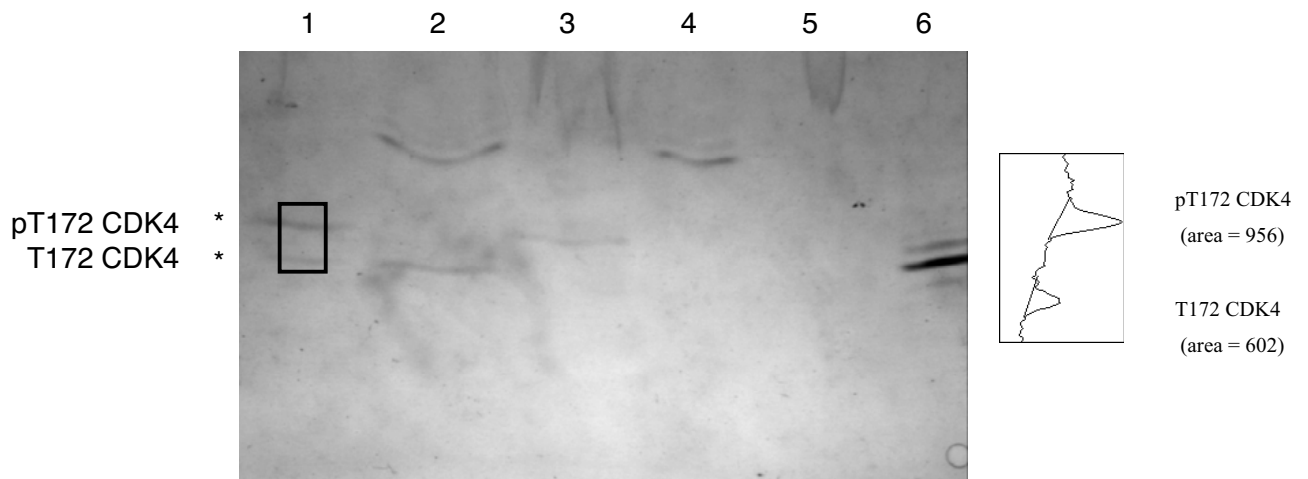
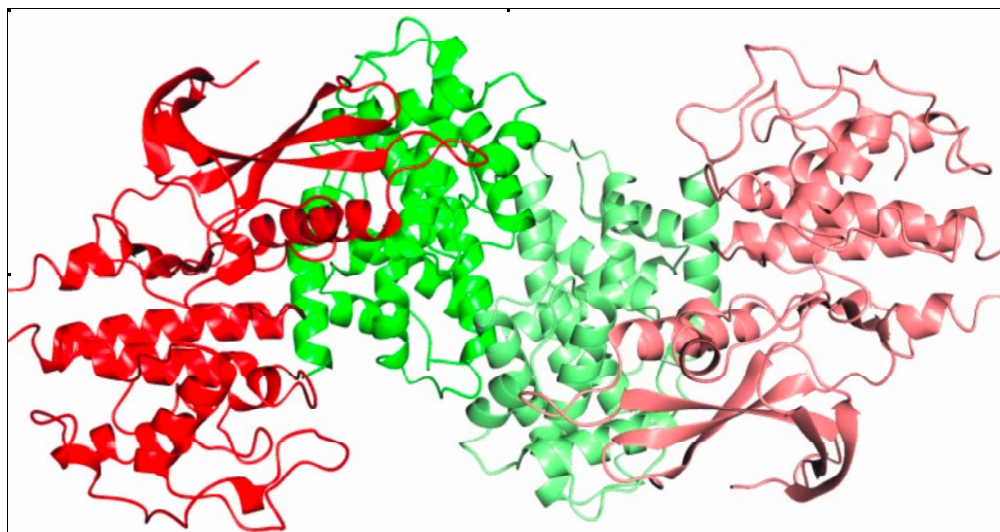


Fig. S3. NEpHGE of CDK4/cyclin D3. (A) Analysis by NEpHGE of CDK4/cyclin D3 prepared by coexpression in insect cells shows that the CDK4 is a mixture of phosphorylated and nonphosphorylated forms (lane 1, pI CDK4 6.52, pI cyclin D3 4.97). Treatment with λ phosphatase (lane 2) or CDK7/cyclin H (lane 3) results, respectively, in fully nonphosphorylated or phosphorylated CDK4. Lane 4, λ phosphatase (pI 5.49); lane 5, CDK7/cyclin H; lane 6, carbonic anhydrase marker (pI 6.5). (B) Densitometric profile of the boxed region in lane 1 of A. Peak areas corresponding to the phosphorylated species (upper band) and unphosphorylated species (lower band) were 956 and 602, respectively.

A



B

Formula	Composition	Surface area, sq. Å	Buried area, sq. Å	ΔG^{int} , kcal/mol	ΔG^{diss} , Kcal/mol
A_2B_2	ABCD	46510	7420	-33.6	2.2
AB	CB	24600	2280	-10.9	2.7
AB	AD	24790	2250	-10.9	1.3
A_2	BD	21450	2880	-11.8	6.2

C

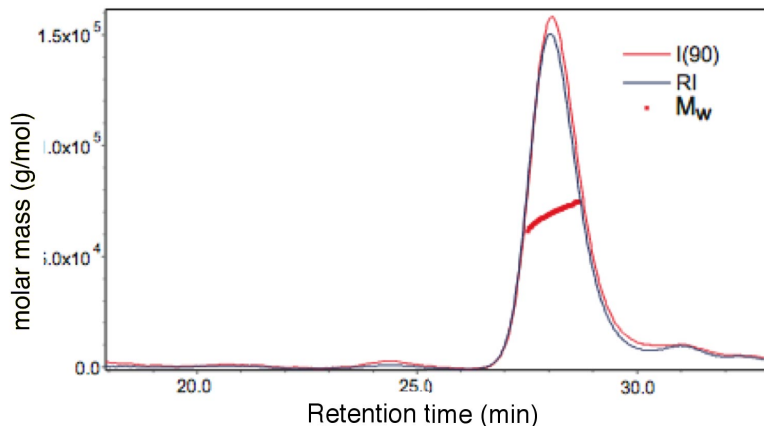


Fig. S5. CDK4/cyclin D3 solution and crystal properties. (A) CDK4/cyclin D3 crystallizes as a dimer. CDK4/cyclin D3 crystals contain a CDK4/cyclin D3 dimer in the crystallographic asymmetric unit. The 2 CDK4/cyclin D3 dimers are drawn in ribbon representation with CDK4 and cyclin D3 subunits colored red and green, respectively. To form the dimer, the cyclin C-terminal sequence (including the C-helix) needs to undergo substantial structural rearrangement (see *Results* for details). (B) CDK4/cyclin D3 intermolecular interface analysis. The intermolecular interfaces within the CDK4/cyclin D3 crystals were analyzed using the PISA server available through the European Bioinformatics Institute (1). Within the lattice, molecules A and C are CDK4, B and D are cyclin D3. (C) CDK4/cyclin D3 is a dimer in solution. The solution molecular weight of the CDK4/cyclin D3 complex was determined by using size-exclusion chromatography coupled to multiangle laser light scattering (SEC-MALLS). The elution profile produced by application of 250 μg (0.24 mg/mL) of CDK4/cyclin D to a Superdex 200 10/300. The blue line is the chromatogram recorded by the differential refractometer, and the red line is the chromatogram recorded from the intensity of scattered light at 90°. Overlaid points in red are individual measurements of the weight-averaged molecular weight determined at 1-s intervals throughout the elution of chromatographic peaks using the ASTRA software. Despite the formation of an extensive cyclinD3–cyclin D3 interface within the crystals, CDK4/cyclin D3 is a dimer in solution.

1. Krissinel E, Henrick K (2007) Inference of macromolecular assemblies from crystalline state. *J Mol Biol* 372:774–797.

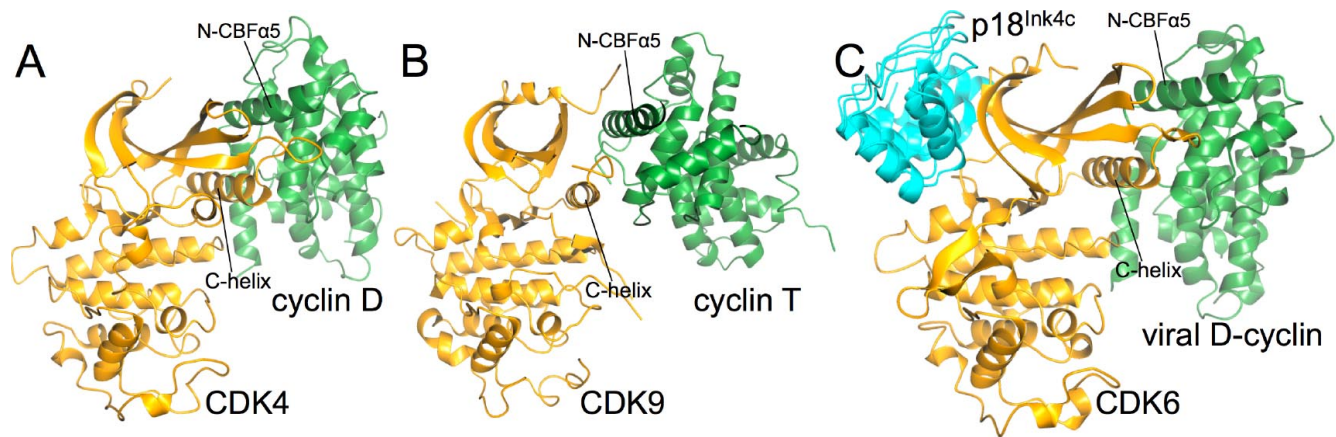


Fig. 57. Comparison of the structure of CDK4/cyclin D3 with other CDK/cyclin complexes. (A) CDK4/cyclin D3. (B) CDK9/cyclin T1. (C) CDK6/p18^{Ink4c}/viral D-cyclin. The CDK is colored gold and the cyclin subunit is green. The CDK inhibitor p18^{Ink4c} in C is colored cyan. Each picture is taken from the same viewpoint with respect to the CDK subunit and for comparison this is the same as that used to generate Fig. 1. CDK9/cyclin T1 and CDK6/p18^{Ink4c}/K-cyclin PDB ID codes are 3BLH and 1G3N respectively.

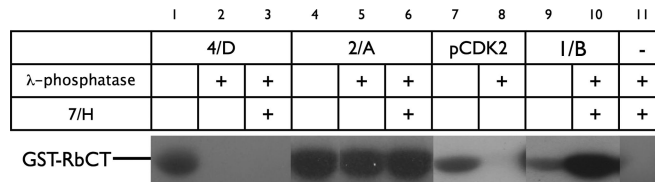


Fig. S8. CDK/cyclin activation monitored by enhanced activity towards GST-pRbCT. Selected CDK/cyclin complexes were sequentially incubated with I phosphatase and CDK7/cyclin H and activation monitored by their resulting activity towards a C-terminal fragment of pRb. Partially T172-phosphorylated CDK4/cyclin D3, as purified from insect cells, is active as a GST-pRbCT kinase (lane 1). Treatment with I phosphatase fully inactivates CDK4/cyclin D3 (lane 2). Despite prolonged coincubation, phosphatase-treated CDK4/cyclin D3 did not recover GST-RbCT kinase activity after treatment with CDK7/cyclin H (lane 3). Kinase activity of T160pCDK2/cyclin A (lane 4) proved to be resistant to phosphatase treatment (lane 5), and its activity was not enhanced by treatment with CDK7/cyclin H (lane 6). Monomeric T160pCDK2 (lane 7) could be inactivated by phosphatase treatment (lane 8). The CDK1/cyclin B complex is prepared in a predominantly nonphosphorylated form with a relatively low intrinsic activity towards GST-RbCT (lane 9) that can be substantially enhanced by treatment with CDK7/cyclin (lane 10). Phosphatase and 7/H do not of themselves possess GST-pRbCT kinase activity (lane 11).

